https://doi.org/10.1016/j.eswa.2021.115228

A Bi-objective Reliable Path-Finding Algorithm for Battery Electric Vehicle Routing

Xiao-Wei Chen [a,b,c], Bi Yu Chen [a,b,c,*] , William H.K. Lam [a,*] , Mei Lam Tam [a] , Wei Ma [a]

[a] *Department of Civil and Environmental Engineering, The Hong Kong Polytechnic University, Hung Hom, Kowloon, Hong Kong, China*
[b] *State Key Laboratory of Information Engineering in Surveying, Mapping and Remote Sensing, Wuhan University, Wuhan 430079, China*
[c] *Collaborative Innovation Center of Geospatial Technology, Wuhan 430079, China*

* Corresponding author

E-mail addresses: vision0823@163.com (X.-W. Chen), chen.biyu@whu.edu.cn (B.Y. Chen), william.lam@polyu.edu.hk (W.H.K. Lam), trptam@polyu.edu.hk (M.L. Tam), wei.w.ma@polyu.edu.hk (W. Ma)

Abstract: This paper proposes a bi-objective reliable path-finding algorithm for routing battery electric vehicles on a road network, with vehicles' energy consumption uncertainty and travel time uncertainty. A bi-objective stochastic optimization problem is proposed and formulated to simultaneously maximize energy consumption reliability (ECR) and travel time reliability (TTR). ECR is defined as the probability of finishing a trip without exhausting a given battery energy budget, while TTR is the on-time arrival probability with the travel time budget. In this study, the proposed optimization problem is decomposed into two sub-problems: (1) finding K most reliable paths for maximizing the TTR objective and (2) finding the most reliable path for optimizing the ECR objective. Then, a novel ranking algorithm is proposed to exactly solve the formulated optimization problem. A case study is carried out on Hong Kong's road network to demonstrate the efficacy and efficiency of the proposed algorithm for real-world applications.

Keywords: Bi-objective path finding; travel time reliability; energy consumption reliability; network uncertainties

1. Introduction

In recent years, worsening environmental problems and the rising price of oil have led to battery electric vehicles (BEVs) becoming increasingly popular. However, compared with traditional fuel vehicles, BEVs usually require a long time to be fully recharged and their charging facilities are less accessible (Shen et al., 2019). As a result, multiple objectives, e.g., energy consumption and travel times, may need to be considered by BEV users making path-choice decisions. Thus, there is a great need to develop multi-objective path-finding algorithms to aid BEV users in making complicated path-choice decisions, particularly for congested road networks with different sources of uncertainties. This paper addresses this bi-objective path-finding problem (PFP) in stochastic networks wherein a range of uncertainties exist.

`

In the literature, PFPs for traditional fuel vehicles in deterministic networks have been intensively studied over the past 50 years (Dijkstra, 1959; Li et al., 2015). In recent years, there has been a resurgence of interest in PFPs in stochastic networks with travel time uncertainties that are commonly encountered in realistic road networks, such as those due to traffic accidents or bad weather (Jiang & Szeto, 2016; Lam, Shao, & Sumalee, 2008; Shao, Lam, & Tam, 2006; Tan, Yang, & Guo, 2014). Many empirical studies have shown that travel time uncertainties have significant effects on travelers' route-choice behaviors (Chen, et al., 2012; Lam & Small, 2001; Li, Huang, & Lam, 2012; Wu & Nie, 2011). Faced with travel time uncertainties, travelers tend to become risk-averse (Beaud, Blayac, & Stephan, 2016; Engelson & Fosgerau, 2016). That is, they choose a reliable path despite its extra travel time budget to ensure a higher probability of their on-time arrival, a parameter that is denoted as travel time reliability (TTR). This behavior has led to TTR being explicitly considered in many studies. Several reliable path-finding models have been fully developed, with the most reliable model (Frank, 1969) and the α-reliable model (Chen & Ji, 2005; Chen et al., 2018; Ji, Kim, & Chen, 2011) being the two most commonly used. The most reliable model finds the optimal path by maximizing TTR for a given travel time budget. The α-reliable model determines the optimal path by minimizing the travel time budget while satisfying a TTR constraint α. Based on these models, several effective and efficient solution algorithms have been developed (Chen et al., 2012; Chen, et al., 2013a; Chen, Li, & Lam, 2016; Chen et al., 2020; Nie & Wu, 2009).

More attention has recently focused on developing path-finding algorithms for BEVs (Shen et al., 2019). Several effective energy consumption formulas have been proposed that take into account various factors which influence the energy consumption of BEVs, such as speed, slope, BEV mass, travel distance, and energy dissipated and recovered during acceleration and deceleration phases (Faraj & Basir, 2016; He, Yin, & Lawphongpanich, 2014; Yang et al., 2014; Zhang & Yao, 2015). Based on these formulas, many solution algorithms have been developed to identify the energy-optimal path. Frank, Castignani, Schmitz, and Engel (2013) presented an eco-driving application which considered drivers' energy-efficient driving attitude. Kluge et al. (2013) empirically determined that the average energy consumption associated with energy-optimal paths is approximately 10% less than the average energy consumption associated with fastest paths. Shen et al. (2019) presented a model that finds the energy-optimal paths using two different energy consumption formulas. However, these path-finding algorithms do not consider the effects of travel-speed variations and associated energy consumption uncertainties.

To the best of our knowledge, there has been little attention paid in the literature to the development of path-finding algorithms for BEVs in stochastic road networks, with the notable exception of Jafari and Boyles (2017). In their study, the energy consumption of a BEV on a link was explicitly formulated as a random variable by using a simplified linear function of link length and random speed variables. A solution algorithm was then developed to find the optimal path by maximizing energy consumption reliability (ECR), which is defined as the probability of finishing the trip without exhausting a given energy budget. However, their energy consumption formulas can be further extended to improve the BEVs' energy consumption phases (such as taking into account energy consumption due to uphill resistance and acceleration resistance) and to consider the BEVs' energy recovery phases. Apart from their PFP algorithm for the optimization of the ECR objective only, other alternative path-finding objectives such as TTR should also be incorporated, particularly in congested road networks with uncertainties in travel times.

This study aims to develop a bi-objective reliable path-finding algorithm for the routing of BEVs on road networks with energy consumption uncertainty and travel time uncertainty. A bi-

`

objective stochastic optimization model is proposed and formulated to simultaneously maximize ECR and TTR. A new ranking algorithm is developed to exactly solve the formulated optimization model. This study extends previous studies in the following aspects. First, a comprehensive stochastic energy consumption formula is developed. The developed energy consumption formula is a stochastic extension of the state-of-the-art deterministic formulas (Faraj & Basir, 2016; Shen et al., 2019). Therefore, it extends the previous stochastic energy consumption formulas (Jafari & Boyles, 2017) by explicitly considering uncertainties during various energy consumption and recovery phases. Second, a novel ranking algorithm is developed to exactly solve the proposed bi-objective stochastic optimization model. The proposed model cannot be solved using the existing bi-objective shortest path-finding algorithms (Skriver, 2000; Raith & Ehrgott, 2009) due to the non-additive property of the objectives considered in this paper. The developed ranking algorithm decomposes such an optimization problem into two sub-problems: (1) finding the K most reliable paths for the TTR objective, and (2) finding the most reliable path for the ECR objective. Two effective procedures are proposed to exactly solve the two sub-problems. The optimization of the developed ranking algorithm is rigorously proved together with the associated properties. Therefore, the developed algorithm enriches the previous related studies (Skriver, 2000; Raith & Ehrgott, 2009) by solving the bi-objective stochastic optimization problems with non-additive properties. Third, a realistic case study is carried out using real traffic data collected in Hong Kong. The results of the case study illustrate the efficacy and efficiency of the proposed algorithm for real-world applications.

2. Model formulations

2.1. Model assumptions

A1. Link travel speeds are assumed to follow independent normal distributions (Lam, Chan, & Shi, 2002).
A2. Link travel times are the reciprocal of normal distributions, which can be approximated as lognormal distributions (Chen et al., 2013a; 2013b). The path travel times also follow lognormal distributions.
A3. If the link upstream travel speed is lower than the downstream travel speed, the vehicle will accelerate at a fixed acceleration; otherwise, the vehicle will decelerate at a fixed negative acceleration.
A4. If a road link is downhill, the vehicle on that link will brake to maintain a stable speed.

2.2. TTR objective

Consider a directed network $\mathrm{G(N, A)}$, consisting of a set of nodes N and a set of links A. Each link $a_{ij} \in A$, from the tail node i to the head node j, has a random travel speed V_{ij} which is assumed to follow a normal distribution (see Assumption A1), with its mean and standard deviation (SD) denoted by v_{ij} and σ_{ij}^{v}, respectively. Let d_{ij} be the length of link a_{ij}. Accordingly, the link travel time, denoted by T_{ij}, can be expressed as follows:

$$T_{ij} = d_{ij}/V_{ij} \tag{1}$$

`

According to Chen et al. (2013b), T_{ij}, the reciprocal of the normal distribution, can be well approximated by a lognormal distribution. Its mean t_{ij} and SD σ_{ij}^{t} can be calculated as follows:

$$t_{ij} = d_{ij}/v_{ij} \tag{2}$$

$$\sigma_{ij}^{T} = \sqrt{d_{ij}\sigma_{ij}^{v}/(v_{ij})^2} \tag{3}$$

For each node $i \in$ N, the successor nodes and predecessor nodes of node n_i are represented as SUCC(i) and PRED(i), respectively, and the elevation is denoted by h_i.

Let P^{rs} be the set of all paths from origin r to destination s. A path $p_i^{rs} \in P^{rs}$ consists of a set of links. The path travel time, denoted by $T_{p_i}^{rs}$, can be calculated as the sum of link travel times along the path, as follows:

$$T_{p_i}^{rs} = \sum_{\forall a_{ij} \in A} T_{ij}\, x_{ij}^{rs} \tag{4}$$

where x_{ij}^{rs} is a binary variable, $x_{ij}^{rs} = 1$ means that link a_{ij} is on path p_i^{rs}, and $x_{ij}^{rs} = 0$ otherwise. As link travel times follow a lognormal distribution, the path travel time distribution does not have a closed-form. Following the work of Kaparias, Bell, and Belzner (2008), it is assumed that the path travel time, $T_{p_i}^{rs}$, follows a lognormal distribution (see Assumption A2). Many empirical studies have also reported that path travel time distributions can be well represented by lognormal distributions (Chen et al., 2013a). Let $t_{p_i}^{rs}$ and $\sigma_{p_i}^{rs}$ be the mean and SD of $T_{p_i}^{rs}$, respectively. These can be calculated as follows:

$$t_{p_i}^{rs} = \sum_{\forall a_{ij} \in A} t_{ij}\, x_{ij}^{rs} \tag{5}$$

$$\sigma_{p_i}^{rs} = \sqrt{\sum_{\forall a_{ij} \in A} (\sigma_{ij}^{T})^2 x_{ij}^{rs}} \tag{6}$$

The distribution of path travel time $T_{p_i}^{rs}$ can be expressed as $T_{p_i}^{rs} \sim Log\text{-}N(u_{p_i}^{T}, sd_{p_i}^{T})$, where $u_{p_i}^{T}$ and $sd_{p_i}^{T}$ are the mean and SD of the natural logarithm of path travel time, respectively. These are given by the following relationships with $t_{p_i}^{rs}$ and $\sigma_{p_i}^{rs}$:

$$sd_{p_i}^{T} = [\ln\left(1 + (\sigma_{p_i}^{rs})^2/(t_{p_i}^{rs})^2\right)]^{1/2} \tag{7}$$

$$u_{p_i}^{T} = \ln\left(t_{p_i}^{rs}\right) - 0.5\left(sd_{p_i}^{T}\right)^2 \tag{8}$$

Therefore, TTR (i.e., the probability of arriving at the destination before a given travel time budget t_0) denoted by $R_{p_i}^{T}$, is expressed as follows:

$$R_{p_i}^{T} = \Phi\left(\frac{\ln(t_0) - u_{p_i}^{T}}{sd_{p_i}^{T}}\right) \tag{9}$$

where $\Phi(\cdot)$ is the cumulative distribution function (CDF) of the standard normal distribution.

In this paper, the first objective (Eq. (9)) of the reliable PFP is to identify the optimal reliable path to maximize TTR within a given travel time budget t_0. The threshold t_0 is a specified travel time buffer that is required by travelers to allow a safety margin against the travel time uncertainty for their travel between a given origin and destination (OD) pair.

2.3. ECR objective

In recent years, researchers have proposed several formulas to estimate the energy consumption of BEVs. Most formulas are based on the vehicle dynamics model, with consideration of the braking process (Yang et al., 2014; Zhang and Yao, 2015; Faraj et al., 2016; Baek et al., 2019). A simple example shown in Fig. 1 is used to illustrate BEV operation. During

`

the entire process, the energy of a BEV consists of two components: energy consumed due to resistance and energy recovered due to regenerative braking.

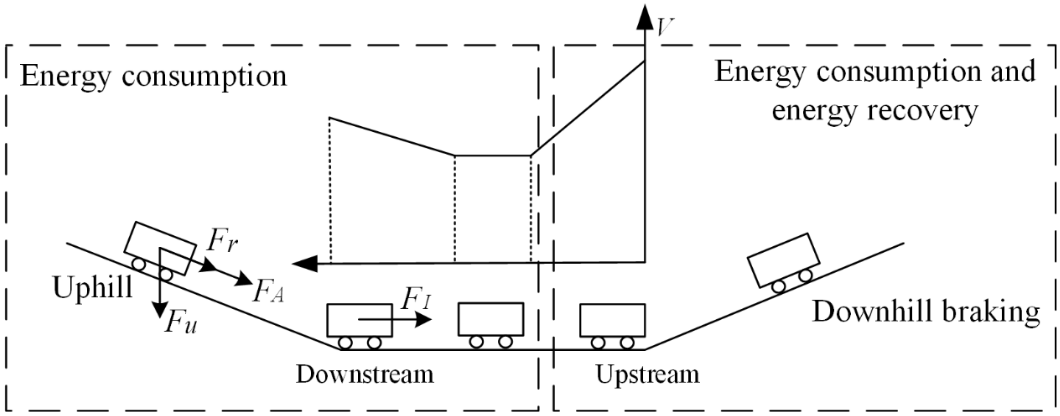

Fig. 1. Process of BEV operation.

As shown in Fig. 1, the applied resistance acting on a BEV in the longitudinal direction consists of four components in general: rolling resistance F_r, aerodynamic resistance F_A, uphill resistance F_u, and acceleration resistance F_I. Hence, the energy consumption of a link a_{ij}, denoted by C_{ij}, is expressed by four corresponding components: loss of energy due to rolling resistance (denoted by $c_{ij,r}$), loss of energy due to aerodynamic resistance (denoted by $C_{ij,A}$), energy consumed due to uphill resistance (denoted by $c_{ij,u}$), and energy consumed due to acceleration resistance (denoted by $C_{ij,I}$). They can be calculated by:

$$c_{ij,r} = \frac{1}{\eta_c \eta_m} \varepsilon_r mg \cos\theta \, d_{ij} \tag{10a}$$

$$C_{ij,A} = \frac{1}{\eta_c \eta_m} \frac{1}{2} \rho \varepsilon_0 \varepsilon_a d_{ij} (V_{ij})^2 \tag{10b}$$

$$c_{ij,u} = \begin{cases} \frac{1}{\eta_c \eta_m} mg(h_j - h_i), & if\ h_j > h_i \\ 0, & if\ h_j < h_i \end{cases} \tag{10c}$$

$$C_{ij,I} = \frac{1}{\eta_c \eta_m} \delta m a V_{ij} t_A \tag{10d}$$

where ε_r is the rolling-resistance coefficient, m is the BEV mass, g is the gravitational acceleration factor, θ is the road gradient (which can be calculated by elevation), ρ is the air density, ε_0 is the aerodynamic drag coefficient, ε_a is the frontal area of the BEV, a is the acceleration, η_c and η_m represent the controller efficiency and motor efficiency, respectively, δ is a coefficient that is related to the BEV mass, and t_A is the travel time during the vehicle acceleration phase. If a link is a downhill, $c_{ij,u}$ equals zero. The energy consumed by accessories (e.g., an air conditioner) is not considered explicitly in this paper, as the aim is to generally illustrate the essential ideas.

During the braking process, energy can be recovered, i.e., regenerated. This regenerated energy consists of downhill regenerative energy (denoted by $c_{ij,d}$) and deceleration regenerative energy (denoted by $c_{ij,de}$). Both $c_{ij,d}$ and $c_{ij,de}$ can be expressed by:

$$c_{ij,d} = \begin{cases} \eta_c \eta_m mg(h_i - h_j), & if\ h_i > h_j \\ 0, & if\ h_i \le h_j \end{cases} \tag{11a}$$

`

$$c_{ij,de} = k\eta_c\eta_m\left(\varepsilon_r mg\cos\theta + \frac{1}{2}\rho\varepsilon_0\varepsilon_a v_{ij}^2 + mg\sin\theta + \delta ma\right)v_{ij}t_D \tag{11b}$$

where k is the regenerative braking factor, which indicates the percentage of the energy that can be recovered by the motor, and t_D is the travel time during the vehicle deceleration phase. To simplify the calculation of energy consumption due to acceleration and deceleration, the fixed acceleration a is used and energy consumption variation during the deceleration phase is not considered (based on Assumptions A3 and A4).

Thus, the energy consumption of link a_{ij} can be expressed by:

$$C_{ij} = c_{ij,r} + c_{ij,u} + C_{ij,A} + C_{ij,I} - c_{ij,de} - c_{ij,d} \tag{12}$$

Clearly, four components, i.e., $c_{ij,r}$, $c_{ij,u}$, $c_{ij,de}$, and $c_{ij,d}$, are deterministic variables that are identical to the previous study (Shen et al., 2019). Nevertheless, the other two components, i.e., $C_{ij,A}$ and $C_{ij,I}$, are random variables that are a stochastic extension of the previous study (Shen et al., 2019) by replacing deterministic speed v_{ij} with speed distribution V_{ij}. Because V_{ij} is assumed to follow normal distributions, the mean and SD of $C_{ij,A}$ can be expressed as:

$$u_{ij}^A = \frac{1}{2\eta_c\eta_m}\rho\varepsilon_0\varepsilon_a((v_{ij})^2 + (\sigma_{ij}^v)^2)d_{ij} \tag{13a}$$

$$\sigma_{ij}^A = \frac{1}{2\eta_c\eta_m}\rho\varepsilon_0\varepsilon_a d_{ij}\sqrt{4{v_{ij}}^2(\sigma_{ij}^v)^2 + 2(\sigma_{ij}^v)^4} \tag{13b}$$

Similarly, the mean and SD of $C_{ij,I}$ can be expressed as:

$$u_{ij}^I = \frac{1}{\eta_c\eta_m}\delta mat_A v_{ij} \tag{13c}$$

$$\sigma_{ij}^I = \frac{1}{\eta_c\eta_m}\delta mat_A\sigma_{ij}^v \tag{13d}$$

Let u_{ij}^c and σ_{ij}^c be mean and SD of link energy consumption C_{ij}, respectively. They can be calculated as follows:

$$u_{ij}^c = c_{ij,r} + c_{ij,u} - c_{ij,de} - c_{ij,d} + u_{ij}^A + u_{ij}^I \tag{14a}$$

$$\sigma_{ij}^c = \sqrt{(\sigma_{ij}^A)^2 + (\sigma_{ij}^I)^2} \tag{14b}$$

The energy consumption distribution along path p_i^{rs}, denoted by $C_{p_i}^{rs}$, is assumed to approximately follow a normal distribution. Thus, based on Assumptions A3 and A4, its mean $u_{p_i}^C$ and SD $\sigma_{p_i}^C$ are expressed as follows:

$$u_{p_i}^C = \sum_{a_{ij}\in A} u_{ij}^c x_{ij}^{rs} \tag{15a}$$

$$\sigma_{p_i}^C = \sqrt{\sum_{a_{ij}\in A}(\sigma_{ij}^c)^2\, x_{ij}^{rs}} \tag{15b}$$

Hence, ECR $R_{p_i}^C$ (i.e., the probability of finishing the trip without running out of a given energy budget e_0) is expressed as follows:

$$R_{p_i}^C = \Phi\left(\left(e_0 - u_{p_i}^C\right)/\sigma_{p_i}^C\right) \tag{16}$$

The second objective, Eq. (16), of the reliable PFP is to find the optimal path for the maximization of ECR within a given energy consumption threshold e_0. The threshold e_0 is a perceived energy consumption buffer that is required by travelers to decrease their energy consumption uncertainty for their travel between an OD pair.

2.4. Bi-objective reliable PFP

`

In view of the above objectives, bi-objective reliable PFP is formulated as the following bi-objective minimization problem:

Maximize: $(R_{p_i}^T, R_{p_i}^C)$ (17a)

Subject to:

$$\sum_{j\in \mathrm{SUCC}(i)} x_{ij}^{rs} - \sum_{q\in \mathrm{PRED}(i)} x_{qi}^{rs} = \begin{cases} 1, & \forall i = r \\ 0, \forall i \neq r, \forall i \neq s \\ -1, & \forall i = s \end{cases} \quad (17b)$$

$$x_{ij}^{rs} \in \{0,1\}, \forall a_{ij} \in A \quad (17c)$$

where Eq. (17a) is the bi-objectives of which travelers aim to maximize simultaneously; Eq. (17b) ensures that links on a path are feasible; and Eq. (17c) is concerned with the link-path incidence variables which are binary in nature.

Definition 1. Given two paths $p_i^{rs} \in P^{rs}$ and $p_j \in P^{rs}$, p_i^{rs} dominates p_j^{rs} if and only if (i) $R_{p_i}^T > R_{p_j}^T$ and $R_{p_i}^C \geq R_{p_j}^C$ or (ii) $R_{p_i}^T \geq R_{p_j}^T$ and $R_{p_i}^C > R_{p_j}^C$ are satisfied.

Definition 2. A path p_i^{rs} is a non-dominated path, if and only if p_i^{rs} is not dominated by any path $p_j^{rs} \in P^{rs}$.

A solution to solve this problem is a set of all non-dominated paths with respect to the bi-objectives (17a). In the next section, a solution algorithm is proposed to exactly solve such a problem.

3. Solution algorithm

In the literature, several solution algorithms have been proposed to exactly solve the traditional additive bi-objective PFPs. For example, the ranking method (Skriver, 2000) is used to determine the non-dominated paths by calculating K shortest paths with respect to each additive objective. However, these algorithms cannot be used to solve the proposed bi-objective reliable PFP, because of the non-additive property of TTR (Eq. (9)) and ECR (Eq. (16)). In this study, a new ranking algorithm is proposed to exactly solve the proposed bi-objective reliable PFP. The proposed algorithm consists of two major procedures: (1) finding K most reliable paths for the TTR objective, and (2) finding the most reliable path for the ECR objective.

3.1. Procedure for finding K most reliable paths for the TTR objective

This section presents a method for finding K most reliable paths with respect to the TTR objective. By substituting Eq. (7) and Eq. (8) into the TTR formulation, Eq. (9), the TTR for path p_i^{rs}, can be rewritten as follows:

$$R_{p_i}^T = \Phi\left[\frac{\ln(t_0/t_{p_i}^{rs})}{\left(\ln\left(1+(\sigma_{p_i}^{rs})^2/(t_{p_i}^{rs})^2\right)\right)^{0.5}} + 0.5 sd_{p_i}^T\right] \quad (18)$$

Let $\sigma_{min}^T = min_{p\epsilon P^{rs}}\left(\sigma_p^{rs}\right)$ be the least SD of path travel time distribution among all paths in P^{rs}; and $sd_{max}^T = max_{a_{ij}\epsilon A}\left(sd_{ij}^T\right)$ be the largest SD of underlying normal distribution for any link on the network. By replacing $\sigma_{p_i}^{rs}$ and $sd_{p_i}^T$ with σ_{min}^T and sd_{max}^T, the upper bound, denoted by $UB\left(R_{p_i}^T\right)$, of the TTR objective can be constructed as:

`

$$UB\left(R_{p_i}^T\right) = \Phi\left[\frac{\ln(t_0/t_{p_i}^{rs})}{\left(\ln\left(1+(\sigma_{min}^T)^2/(t_{p_i}^{rs})^2\right)\right)^{0.5}} + 0.5sd_{max}^T\right] \tag{19}$$

The proof of the $UB\left(R_{p_i}^T\right) \geq R_{p_i}^T$ relationship is given in Proposition A2 (see Appendix). Since σ_{min}^T and sd_{max}^T are fixed, this upper bound $UB\left(R_{p_i}^T\right)$ is the function of only the mean path travel time $t_{p_i}^{rs}$. We can prove that $UB\left(R_{p_i}^T\right)$ is a monotonically decreasing function of $t_{p_i}^{rs}$ when $t_{p_i}^{rs}$ is greater than $\max(\sigma_{min}^T, t_0/e)$, where e is Euler's number.

Proposition 1. The upper bound $UB\left(R_{p_i}^T\right)$ is a monotonically decreasing function of $t_{p_i}^{rs}$ when $t_{p_i}^{rs} > max(\sigma_{min}^T,\ t_0/e)$ holds.
Proof. See Proposition A3 in the Appendix.

Given the additive property of $t_{p_i}^{rs}$, we can incrementally calculate K shortest paths of $t_{p_i}^{rs}$ by using the classical K shortest path algorithm with t_{ij} as link costs (Yen, 1971). Hence, we can calculate the first shortest paths p_1^t, the second shortest path p_2^t,…, until the k^th^ shortest path p_k^t satisfying $t_{p_k}^{rs} > \max(\sigma_{min}^T, t_0/e)$. After that, the upper bound, $UB\left(R_{p_k}^t\right)$, is a monotonically decreasing function with respect to $t_{p_k}^{rs}$ of the newly calculated k^th^ shortest path. Let P_k^t be the set of calculated k shortest paths with $P_k^t \subseteq P^{rs}$ relationship. For any $p_i^{rs} \in P_k^t$, its actual TTR, $R_{p_i}^t$, can be calculated using Eq. (18). Then, we can determine $max_{p_i \epsilon P_k^t}\left(R_{p_i}^t\right)$ for P_k^t, which is the lower bound, denoted by $LB(R_P^T)$, of the most reliable path in the whole path set P^{rs}. Clearly, this lower bound $LB(R_P^T)$ is a monotonically increasing function with respect to the newly calculated k^th^ shortest path. When $LB(R_P^T) \geq UB\left(R_{p_k}^t\right)$ meets, we can identify the first most reliable path, denoted by $p_{R_1}^T$, for the TTR objective as the path $p_{LB}^T \in P_k^t$ providing the lower bound, i.e., $R_{p_{LB}}^T = LB(R_P^T)$. Then, we can remove p_{LB}^T from P_k^t and update the lower bound, $LB(R_P^T)$. By incrementally calculating k shortest paths, $LB(R_P^T) \geq UB\left(R_{p_k}^t\right)$ meets again. In this way, the second most reliable path, $p_{R_2}^T$,…, until the K^{th} most reliable path, $p_{R_K}^T$, can be determined. This method of finding K most reliable paths for the TTR objective is implemented in the FindKMRP-TTR procedure. Its detailed steps are given in Table 1.

Table 1 Detailed steps of the FindKMRP-TTR procedure.

Input: origin o, destination d, travel time budget t_0, pre-given K, and threshold K_{max}.
Return: Set of K most reliable paths P^T, and set of calculated paths P_k^t.
01: Call *InitializeKMRP-TTR*(o, d, t_0, K_{max}).
02: Set $j \coloneqq 1$.
03: Call *FindNextReliablePath-TTR* to determine the j^th^ most reliable path $p_{R_j}^T$.
04: If $p_{R_j}^T = \emptyset$, then Stop and Return P^T and P_k^t.
05: $P^T \coloneqq P^T \cup \{p_{R_j}^T\}$.
06: If $|P^T| \geq K$ ($|P^T|$ is number of paths in P^T), then Stop and Return P^T and P_k^t.
07: Set $j \coloneqq j + 1$, and Goto Line 03.

Sub-procedure: InitializeKMRP-TTR
Input: origin o, destination d, travel time budget t_0, and threshold K_{max}^T.

01: Determine σ_{min}^T by using a forward one-to-one Dijkstra's algorithm with link travel time variance $(\sigma_{ij}^T)^2$ as link costs.
02: Determine $sd_{max}^T := max_{a_{ij} \epsilon A}\left(sd_{ij}^T\right)$.
03: Set $k := 1$, $P^T \coloneqq \emptyset$ and $P_k^t \coloneqq \emptyset$; and Set $UB\left(R_{p_k}^t\right) := 1$ and $LB(R_P^T) \coloneqq 0$.
04: If $k > K_{max}$, then Stop.
05: Calculate the k^th shortest path p_k^t by using the k shortest path algorithm with t_{ij} as link costs.
06: Add p_k^t into P_k^t, Calculate its $R_{p_k}^t$ using Eq. (18), and Update $LB(R_P^T)$.
07: If $t_{p_k}^{rs} < \max(\sigma_{min}^T, t_0/e)$, then Set $k := k + 1$ and Goto Line 04.

Sub-procedure: FindNextReliablePath-TTR
Return: Reliable path $p_{R_j}^T$.
01: If $LB(R_P^T) \geq UB\left(R_{p_K}^t\right)$ then,
02: Remove lower bound path p_{LB}^{rs} from P_k^t, and Update $LB(R_P^T)$.
03: Stop and Return p_{LB}^{rs}.
04: End if
05: Set $k := k + 1$.
06: If $k > K_{max}$, then Stop and Return $\emptyset$.
07: Calculate the k^th shortest path p_k^t by using the k shortest path algorithm with t_{ij} as link costs.
08: Add p_k^t into P_k^t, Calculate its $R_{p_k}^t$ using Eq. (18), and Update $LB(R_P^T)$.
09: Calculate $UB\left(R_{p_k}^t\right)$ using Eq. (19), and Goto Line 01.

We can prove that, when K_{max} is sufficiently large, the FindKMRP-TTR procedure can guarantee to obtain the K most reliable paths for the TTR objective.

Proposition 2. The FindKMRP-TTR procedure can determine the optimal solution of the K most reliable paths for the TTR objective when K_{max} is sufficiently large.
Proof. See Proposition A4 in the Appendix. □

In this study, the A* technique is further adapted to improve the computational performance of the proposed procedure. Yen's algorithm (Yen, 1971) is a classical algorithm for finding K shortest paths. Yen's (1971) algorithm requires numerous deviation path calculations using the forward one-to-one Dijkstra's algorithm. The A* technique is widely recognized as an effective means for speeding up the one-to-one Dijkstra's algorithm by introducing a heuristic function to assign higher priorities to nodes closer to the destination. The A* technique can achieve the optimal shortest path when the heuristic function is admissible. Therefore, we introduce the A* technique in the classical Yen's algorithm. The used admissible heuristic function is referred to as those shortest path distances from all nodes to the destination, denoted by $t_p(i, d)$, which are pre-calculated using a backward one-to-all Dijkstra's algorithm with t_{ij} as link costs.

3.2. Procedure for finding the most reliable paths for the ECR objective

This section presents a procedure for finding the most reliable path for maximizing the ECR objective. Recently, Chen et al. (2017) proposed an efficient two-stage algorithm, namely MRP-TS, to exactly find the most reliable path when link costs follow independent normal distributions

`

and mean link costs are positive. However, such an algorithm cannot be directly utilized to find the most reliable path for the ECR objective, because u_{ij}^{c} may become negative at certain links where BEVs are running on the energy recovery process. According to the work of Faraj and Basir (2016), the negative link cost issue can be addressed by transforming the weight function u_{ij}^{c} into a positive reduced weighted function $u_{\Pi,ij}^{c}$. Suppose that there are no negative cycles, it can be proven that whenever a potential function Π satisfies the requirement that $\Pi(j) - \Pi(i) \le u_{ij}^{c}$ and $u_{\Pi,ij}^{c}$ is determined as $u_{\Pi,ij}^{c} = u_{ij}^{c} + \Pi(i) - \Pi(j)$, then the optimal routes in the network weighted with $u_{\Pi,ij}^{c}$ are also the optimal routes in the network weighted with u_{ij}^{c} (Faraj & Basir, 2016). The positive reduced weighted function on link a_{ij} and path p_i^{rs} can be expressed as follows:

$$u_{\Pi,ij}^{c} = u_{ij}^{c} + \Pi(i) - \Pi(j) = c_{ij,r} - c_{ij,de} + u_{ij}^{A} + u_{ij}^{I} \tag{20}$$

Therefore, link energy consumption distribution can be expressed as $\check{C}_{ij} \sim N(u_{\Pi,ij}^{c}, \sigma_{ij}^{c})$. Using this transformation technique, we can utilize the MRP-TS algorithm (Chen et al., 2017) to exactly find the most reliable path for the ECR objective.

3.3. Ranking algorithm for solving the bi-objective reliable PFP

This section presents the proposed ranking algorithm, namely FindTtrEcrPathSet, for exactly solving the bi-objective reliable PFP formulated in Section 2.4. The algorithm consists of three steps. In the first step, the algorithm utilizes the MRP-TS algorithm to determine, $p_{R_1}^{C}$, the most reliable path for the ECR objective. The actual TTR of this $p_{R_1}^{C}$ is calculated using Eq. (18) and denoted by R_{Min}^{T}. This R_{Min}^{T} is the lowest TTR for all non-dominated paths, since $R_{p_1}^{C} = max_{p_i \epsilon P^{rs}}\left(R_{p_i}^{C}\right)$ holds. In each iteration of the second step, the j^{th} most reliable path, $p_{R_j}^{T}$, for the TTR objective is incrementally calculated. The actual ECR (denoted by $R_{R_j}^{C}$) of the j$^{\text{th}}$ most reliable path $p_{R_j}^{T}$ is determined using Eq. (16). If this $R_{R_j}^{C}$ is lower than or equal to $R_{R_{j-1}}^{C}$ of the previous $j-1^{\text{th}}$ most reliable path $p_{R_{j-1}}^{T}$, then the j$^{\text{th}}$ most reliable path $p_{R_j}^{T}$ can be discarded, because it is dominated by $p_{R_{j-1}}^{T}$ with $R_{R_j}^{C} \le R_{R_{j-1}}^{C}$ and $R_{R_j}^{T} < R_{R_{j-1}}^{T}$ relationships. Otherwise, this $R_{R_j}^{C}$ is larger than $R_{R_{j-1}}^{C}$, and the j$^{\text{th}}$ most reliable path $p_{R_j}^{T}$ can be identified as a non-dominated path and added into the path set, Ω. The second step terminates when $R_{R_j}^{T} < R_{Min}^{T}$, because all paths with TTR lower than R_{Min}^{T} are obviously dominated by $p_{R_1}^{C}$. In this scenario, the algorithm can obtain the optimal solution, i.e., all non-dominated paths between the OD pair. However, when K_{max} is not sufficiently large, the algorithm can terminate without $p_{R_j}^{T} < R_{Min}^{T}$ and some non-dominated paths may be missed. To mitigate this issue, the third step is introduced to identify potential non-dominated paths in P_K^T (see Section 3.1) by using Definition 1. The detailed steps of the FindTtrEcrPathSet algorithm are given in Table 2.

Table 2 Detailed steps of the FindTtrEcrPathSet algorithm.

Input: origin o, destination d, travel time budget t_0, energy threshold e_0, and threshold K_{max}.
Return: Set of non-dominated paths Ω.
Step 1. Most reliable path finding for the ECR objective:
01: Transform mean energy consumption u_{ij}^{c} of any link into $u_{\Pi,ij}^{c}$ using Eq. (20).
02: Call MRP-TS(o, d, e_0) to find the most reliable path $p_{R_1}^{C}$.

03: Calculate R^T_{Min} as the actual TTR of $p^C_{R_1}$ using Eq. (18).
Step 2. K most reliable path findings for the TTR objective:
04: Call *InitializeKMRP-TTR*(o, d, t_0, K_{max}).
05: Call *FindNextReliablePath-TTR* to determine the first most reliable path $p^T_{R_1}$.
06: If $p^T_{R_1} = \emptyset$, then Set $\Omega := \{\}$ and Goto Line 14.
07: Set $\Omega := \{p^T_{R_1}\}$ and $j := 2$.
08: Call *FindNextReliablePath-TTR* to determine the j^{th} most reliable path $p^T_{R_j}$.
09: If $p^T_{R_j} = \emptyset$, then Goto Line 14.
10: If $R^T_{R_j} < R^T_{Min}$, then Stop and Return Ω.
11: Calculate $R^C_{R_j}$ as the actual ECR for $p^T_{R_j}$ using Eq. (16).
12: If $R^C_{R_j} \leq R^C_{R_{j-1}}$, then Set $j := j + 1$ and Go to Line 08.
13: If $R^C_{R_j} > R^C_{R_{j-1}}$, then $\Omega := \Omega \cup \{p^T_{R_j}\}$, Set $j := j + 1$ and Go to Line 08.
Step 3. Additional non-dominated paths checking:
14: If $p^C_{R_1} \notin \Omega$, then Set $\Omega := \Omega \cup \{p^C_{R_1}\}$.
15: Add potential non-dominated paths in P^T_K, into Ω based on Definition 1.
16: Stop and Return Ω.

We can prove that, when K_{max} is sufficiently large, the proposed FindTtrEcrPathSet algorithm can obtain the optimal solution (i.e., all non-dominated paths) of the bi-objective reliable PFP, as below.

Proposition 4. The FindTtrEcrPathSet algorithm can attain the optimal solution of the bi-objective reliable PFP when K_{max} is sufficiently large.
Proof. See Proposition A5 in the Appendix. □

4. Case study

4.1. Numerical example

This section reports a case study using a real road network in Hong Kong, consisting of 1,367 nodes and 3,655 links (Chen et al., 2013b). The elevation data for all links were extracted from Shuttle Radar Topography Mission (SRTM) – a popular data source of digital elevation models that can be downloaded from (https://srtm.csi.cgiar.org/). The travel speed distributions for all network links were extracted from a Real-time Traveler Information System, RTIS (www.hkemobility.gov.hk/en/traffic-information/live/cctv/all?cctv=on&jt=on&smp=on&ts=on), which was based on real-time traffic data and offline travel times estimated by a traffic flow simulator (Tam & Lam, 2008).

Fig. 2 shows speed distributions for all links in the RTIS network. Fig. 2(a) gives the mean speed, v_{ij}, of every link. In this figure, links shown in red represent congested links (<20 km/h), yellow represents slightly congested links (20–40 km/h), and green represents uncongested links (>40 km/h). It was found that 31.3% of links were congested, and most of them were located in Hong Kong Island. Fig. 2(b) illustrates travel speed uncertainty for all links in the RTIS network. The level of travel speed uncertainty was measured using the coefficient of variation (CV), i.e., the ratio of standard deviation σ_{ij}^{v} to mean v_{ij}. As shown, link travel speeds in the RTIS network were highly stochastic, with the average CV value equal to 0.24. Such travel speed uncertainties indicate large variations in travel times and energy consumption, which should not be ignored for BEV routing.

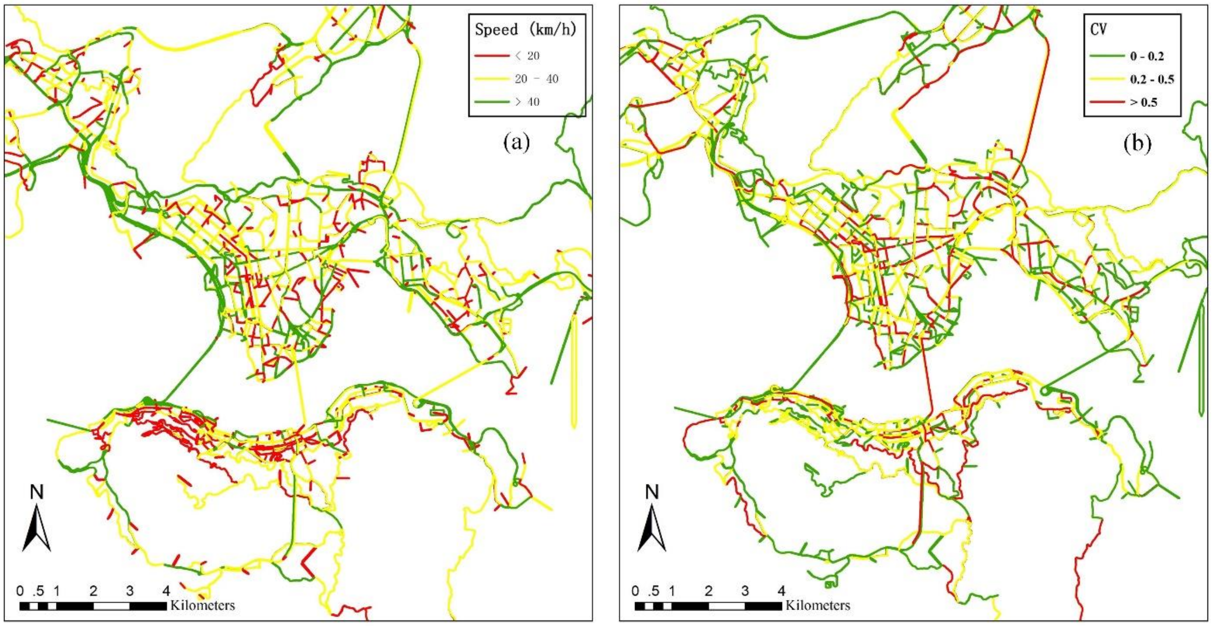

Fig. 2. Link speed distributions for the Hong Kong RTIS road network: (a) mean speed, and (b) coefficient of variation.

We first investigate how different input parameters, travel time budget t_0 and estimated energy consumption threshold e_0, affect the path finding results with respect to the TTR or ECR objective. One OD pair in the RTIS network, from the central business district (CBD) to Richland Gardens (residential estate) in Kowloon Bay (near the old airport), during the PM peak, was chosen as the numerical example. As shown in Fig. 3(a), two paths, i.e., Path 1 and Path 2, were determined as the most reliable paths for the ECR objective under different settings of e_0 parameters. Fig. 3(b) depicts the CDFs of energy consumption distributions for these two paths. When $e_0 = 1.42\ kWh$, Paths 1 and 2 have the same ECR, i.e., 76.35%. As the value of e_0 increases, Path 2 becomes the optimal path, as it has the maximum ECR. For example, when e_0 is increased to 1.53 kWh, Path 1 has the highest ECR, i.e., 90%. Conversely, Path 2 is the optimal path when the value of e_0 decreases. For example, when e_0 decreases to 1.07 kWh, ECR decreases to 20% on Path 2.

Fig. 4(a) shows the most reliable paths for the TTR objective under different travel time budgets, i.e., t_0 parameters. As shown, the optimal paths, Paths 3 and 4, found for the TTR objective were different from Paths 1 and 2 for the ECR objective. The travel time distributions of Paths 3 and 4 are given in Fig. 4(b). It was found that the optimal path was determined by the input t_0 parameter. Paths 3 and 4 can achieve an identical TTR of 37.49% when $t_0 = 18.2$ min. Path 3 was found as the optimal path with TTR = 90% when $t_0 = 19.7$ min, while Path 4 was the optimal path with TTR = 10% when $t_0 = 17.2$ min.

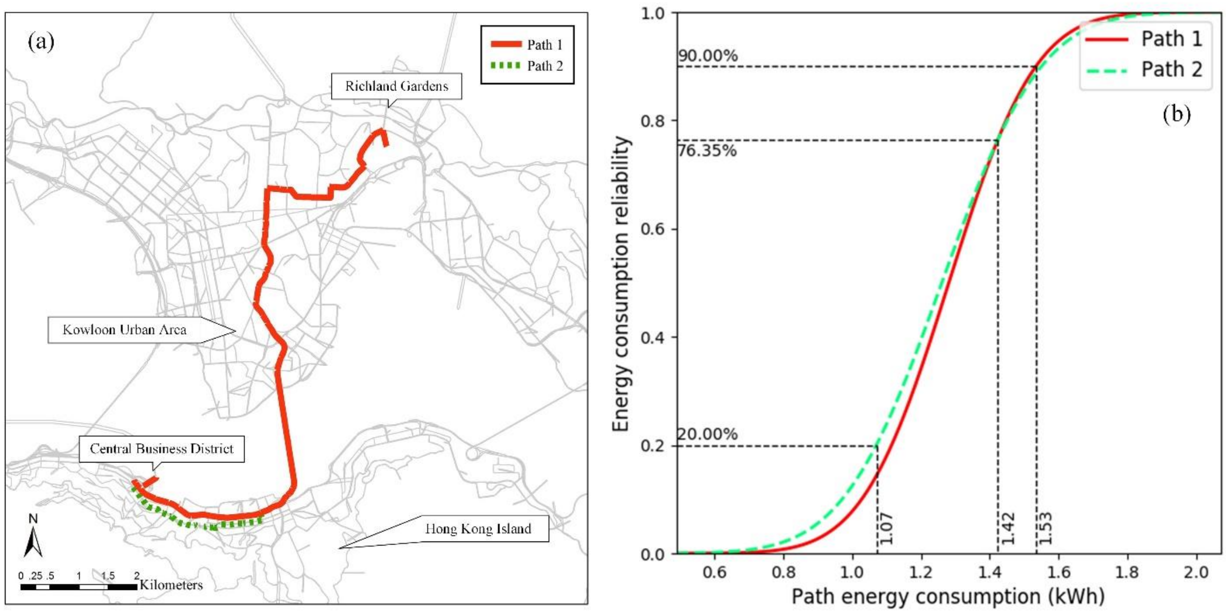

Fig. 3. Two most reliable paths for the energy consumption reliability objective under different e_0 parameters: (a) candidate paths, (b) cumulative distribution functions of path energy consumption.

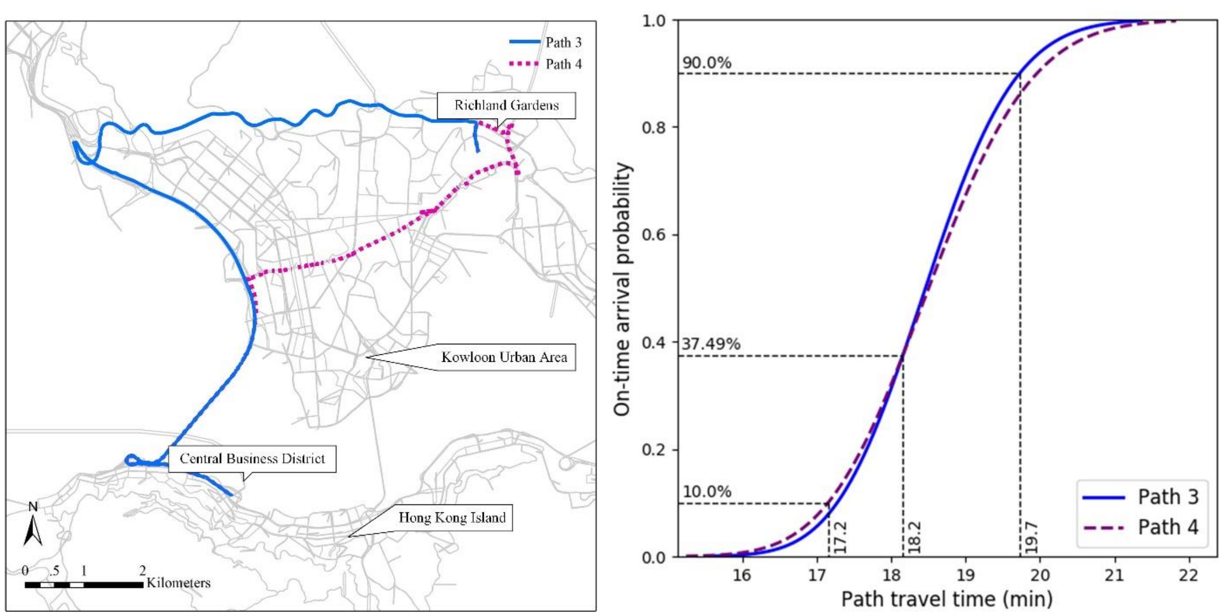

Fig. 4. Two most reliable paths for the travel time reliability objective under different t_0 parameters: (a) candidate paths, (b) cumulative distribution functions of path travel times.

We then investigated the path-finding results of the developed FindTtrEcrPathSet algorithm for simultaneously maximizing both the ECR and TTR objectives between the same OD pair. We set $e_0 = 1.53\ kWh$ and $t_0 = 19.7$ min, so that Path 1 and Path 3 were identified as the most reliable path for ECR = 90% and TTR = 90%, respectively. To make it sufficiently large, we set $K_{max} = 1000$, i.e., the number of calculated k shortest paths of $t_{p_i}^{rs}$ should be less than 1000. For

`

the most reliable path of the ECR objective, i.e., Path 1, its actual TTR can be calculated as $R_{Min}^{T} = 0.658\%$. Fig. 5 shows the bi-objective space for all calculated K most reliable paths for the TTR objective satisfying $R_{R_j}^{T} \geq R_{Min}^{T},\ \forall R_{R_j}^{T} \in P^{T}$. As can be seen, a total of 109 most reliable paths for the TTR objective were determined after 116 shortest paths of $t_{p_i}^{rs}$ were calculated. Among the most reliable paths, only four paths (in red) were identified as non-dominated paths, while 105 paths (in green) were eliminated as dominated paths. These four non-dominated paths are useful solutions, trading off the ECR objective against the TTR objective.

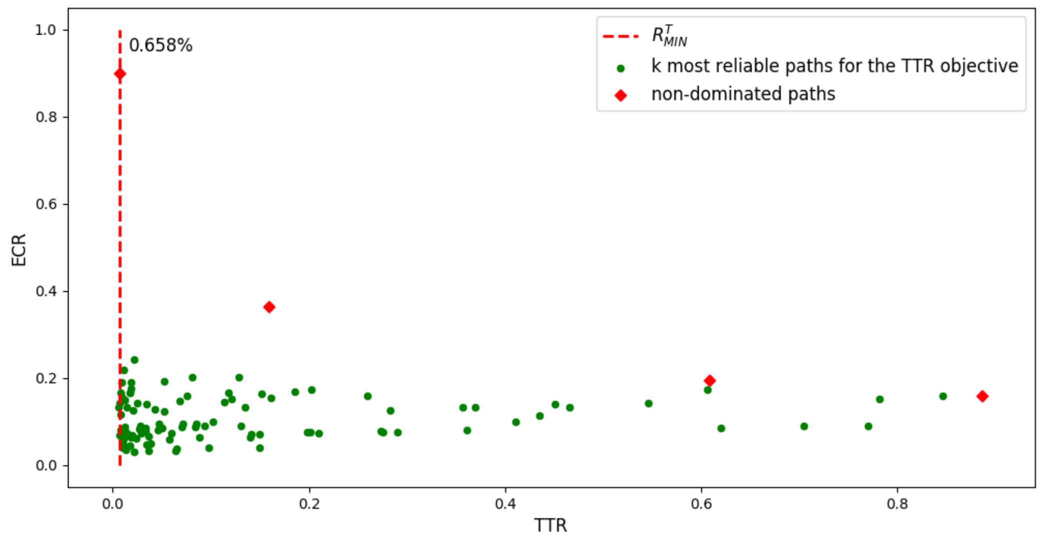

Fig. 5. Solution space for both travel time reliability and energy consumption reliability objectives.

We further investigated how the K_{max} parameter affects the solution accuracy of the developed FindTtrEcrPathSet algorithm. According to Proposition 4, the developed algorithm can achieve the optimal solution, i.e., all non-dominated paths, when K_{max} is sufficiently large. Therefore, we used the non-dominated paths calculated when $K_{max} = 3000$ as the ground truth. The solution accuracy under different K_{max} values was measured using the percentage of actual non-dominated paths determined by the developed algorithm. Fig. 6 shows the solution accuracy using the same OD pair and the same setting of e_0 and t_0 as Fig. 5. As expected, the solution accuracy was improved with the increase of the K_{max} parameter. When $K_{max} = 7$, accuracy of 75% was achieved, i.e., three non-dominated paths were determined. This accuracy reached 100% when $K_{max} = 74$. Fig. 6 also shows the solution accuracy of the developed algorithm without Step 3 (see Table 2). This step was introduced to include $p_{R_1}^{C}$ and identify potential non-dominated paths in P_K^T when K_{max} is not sufficiently large. Thus, such a step can effectively improve the solution accuracy when K_{max} is not sufficiently large.

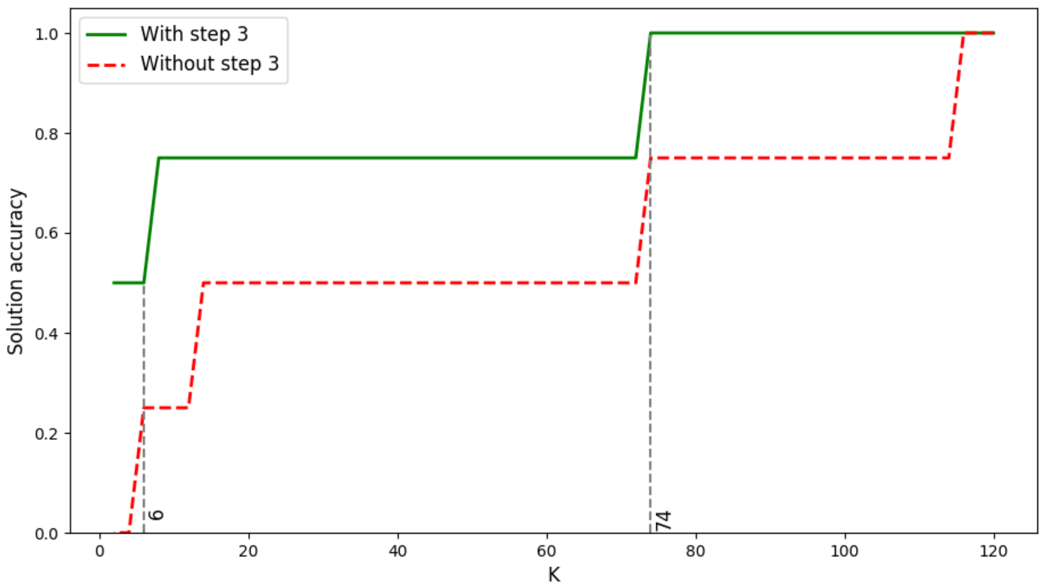

Fig. 6. Solution accuracy of the developed algorithm under K_{max} values.

4.2. Computational performance

The proposed solution algorithm was coded in C# programming language. The F-heap data structure (Fredman & Tarjan, 1987) was used in all shortest path calculation procedures, including Dijkstra's algorithms and the K shortest path algorithms. All of the experiments were conducted on a Windows 8 operating system on a PC equipped with a four-core Intel i5-3230M 2.6 GHz CPU and 8 GB of RAM.

To examine the computational performance of the developed algorithm, we randomly selected 100 OD pairs from the RTIS network. The average computational time for all OD pairs was calculated as an indicator of the computational performance of the developed algorithm. For each OD pair, we calculated the least mean energy consumption path by using one-to-one Dijkstra's algorithm with $u_{\Pi,ij}^{c}$ as link costs. Then, the energy consumption distribution for this calculated path was obtained and its inverse CDF at θ level was set as e_0 parameter for the OD pair. Similarly, we calculated the least travel time path by using one-to-one Dijkstra's algorithm with t_{ij} as link costs. The travel time distribution of this least travel time path was obtained and its inverse CDF at θ level was set as t_0 parameter for the OD pair.

Fig. 7 shows the computational time required by the developed algorithm with the A* technique under different K_{max} values. The parameter $\theta = 90\%$ was used to set the t_0 and e_0 parameters for each OD pair. As expected, the computational times increase nearly in a linear function of K_{max} when K_{max} is small, e.g., $K_{max} < 300$. This is obvious because the larger the number of calculated shortest paths, the greater the computational effort required. The computational performance became relatively stable when K_{max} was large, e.g., $K_{max} > 1000$. This is because optimal solutions had been obtained for most OD pairs before the number of calculated shortest paths reached K_{max} value. Nevertheless, as illustrated in Fig. 6, a small value of K_{max} may reduce solution accuracy. Therefore, a suitable parameter of K_{max} should be set in order to trade off solution accuracy against computational performance.

In this study, the A* technique was adapted to speed up the computational performance for finding K most reliable paths for the TTR objective. To distinguish its effectiveness, the developed

`

algorithm without the A* technique was also implemented for comparison. As can be seen in Fig. 7, the A* technique can significantly speed up the computational performance of the developed algorithm under all K_{max} values. For example, when $K_{max} = 500$, the developed algorithm with the A* technique required 0.43 seconds, which was about 2.67 (1.58 / 0.43 - 1) times faster than that without the A* technique. This computational improvement was achieved due to the utilization of a pre-calculated shortest path tree, i.e., $t_p(i, d)$, as the heuristic function in the K shortest path calculations.

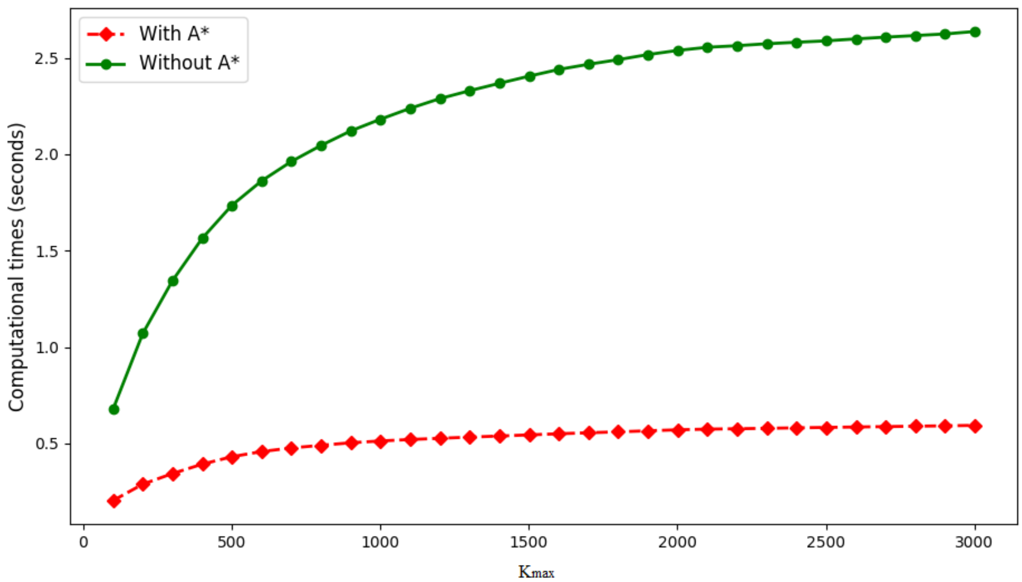

Fig. 7. Computational performance of the developed algorithm under different K_{max} values.

Table 3 shows the computational performance of the developed algorithm with the A* technique under different settings of parameters t_0 and e_0. The values of these two parameters were determined by the θ level. A high-reliability level θ on travel time and energy consumption implies that there is a larger threshold on the travel time budget t_0 and the estimated energy consumption e_0. We set $K_{max} = 500$. As can be seen in Table 3, the computational performance of the developed algorithm was stable under various values of t_0 and e_0, i.e., within 0.5 seconds.

Table 3 Computational performance of the developed algorithm under various values of t_0 and e_0 parameters.

Reliabilities (θ)	**10%**	30%	50%	70%	**90%**
Average computational times (s)	**0.24**	0.28	0.32	0.31	**0.43**
Average number of non-dominated paths	**4.68**	4.73	5.01	5.39	**5.81**

5. Conclusion

This paper proposes a bi-objective reliable path-finding algorithm for the route guidance of BEVs in a road network with travel time and energy consumption uncertainties. A bi-objective stochastic optimization model was proposed and formulated for simultaneously maximizing TTR, i.e., on-time arrival probability with the travel time budget, and ECR, i.e., probability of finishing

`

the journey without exhausting a given energy budget. Due to its non-additive objectives, the proposed model cannot be solved exactly using the existing multi-objective shortest path algorithms built on the additive property of objectives. To address this challenge, the proposed bi-objective reliable path-finding problem was decomposed into two sub-problems: (1) finding K most reliable paths for maximizing the TTR objective, (2) finding the most reliable path for optimizing the ECR objective. A novel ranking algorithm was developed to exactly solve the proposed optimization model. The A* technique was further adapted to improve the efficiency of the developed algorithm. The optimality of the developed algorithm was rigorously proved together with associated properties.

To demonstrate the applicability of the new ranking algorithm, a case study was carried out in Hong Kong using real travel speed distributions collected from RTIS (real-time traveler information system). The path-finding results of the developed algorithm provide a set of non-dominated paths with a trade-off of the TTR objective against the ECR objective. The developed algorithm is able to obtain all non-dominated paths in the RTIS road network when K_{max} is sufficiently large. With the reasonable selection of the K_{max} parameter, the developed algorithm can solve the bi-objective reliable path-finding problem with satisfactory solution accuracy within an acceptable amount of computational time.

The analysis presented in this paper also provides several important insights and policy implications. It was found that travel speeds in road networks can be highly stochastic, leading to high variations in travel times and energy consumption. Travel time budget t_0 and energy consumption threshold e_0, which reflect travelers' assigned resources against travel time and energy consumption uncertainties, significantly affect travelers' route choices – of which planners and policymakers should be aware. Resilient improvements to road network design and service facility location could be achieved by explicitly considering such impacts during planning and design stages (Chen et al., 2019, 2020; Fu et al., 2020).

Several directions for future research are worth noting. First, it was assumed in this study that link travel speeds follow normal distributions and link travel times can be approximated by lognormal distributions. However, the normal distribution of link travel speeds may not always hold in reality. How to incorporate other travel speed distributions, such as gamma or Burr distributions, in the developed algorithm needs further investigation. Second, the correlation between travel time and energy consumption under different vehicle types has not been considered in this study. How to formulate the correlation in travel times and energy consumption by vehicle type and incorporate them into the developed algorithm is warranted for further study. Last but not least, further study should be conducted to consider the dynamics of travel speeds on different days. The extension of the developed algorithm to account for the stochastic dynamic characteristics of travel speeds is certainly another important research direction.

Acknowledgments

The work described in this paper was jointly supported by the National Key Research and Development Program (No. 2017YFB0503600), the Research Grants Council of the Hong Kong Special Administrative Region, China (Project No. PolyU R5029-18), the Dean's Reserve of the Hong Kong Polytechnic University (Project No. ZVSA) and the Natural Science Foundation of Hubei Province (2020CFA054).

`

References

Aljanahi, A. A. M., Rhodes, A. H., & Metcalfe, A. V. (1999). Speed, speed limits and road traffic accidents under free flow conditions. *Accident Analysis and Prevention*, 31, 161-168.

Beaud, M., Blayac, T., & Stephan, M. (2016). The impact of travel time variability and travelers' risk attitudes on the values of time and reliability. *Transportation Research Part B-Methodological*, 93, 207-224.

Ceder, A., & Livneh, M. (1982). Relationships between road accidents and hourly traffic flow - I. Analyses and interpretation. *Accident Analysis and Prevention*, 14, 19-34.

Chen, A., & Ji, Z. (2005). Path finding under uncertainty. *Journal of Advanced Transportation*, 39, 19-37.

Chen, B. Y., Lam, W. H. K., Sumalee, A., & Li, Z. L. (2012). Reliable shortest path finding in stochastic networks with spatial correlated link travel times. *International Journal of Geographical Information Science*, 26, 365-386.

Chen, B. Y., Lam, W. H. K., Li, Q. Q., Sumalee, A., & Yan, K. (2013a). Shortest path finding problem in stochastic time dependent road networks with stochastic first-in-first-out property. *IEEE Transactions on Intelligent Transportation Systems*, 14, 1907-1917.

Chen, B. Y., Lam, W. H. K., Sumalee, A., Li, Q. Q., Shao, H., & Fang, Z. X. (2013b). Finding reliable shortest paths in road networks under uncertainty. *Networks & Spatial Economics*, 13, 123-148.

Chen, B. Y., Li, Q., & Lam, W. H. K. (2016). Finding the k reliable shortest paths under travel time uncertainty. *Transportation Research Part B*, 94, 189-203.

Chen, B.Y., Shi, C., Zhang, J., Lam, W.H.K., Li, Q.Q. & Xiang, S. (2017). Most reliable path-finding algorithm for maximizing on-time arrival probability. *Transportmetrica B*, 5, 253-269.

Chen, B.Y., Wang, Y., Wang, D. and Lam, W.H.K., 2019, Understanding travel time uncertainty impacts on the equity of individual accessibility. *Transportation Research Part D*, 75, pp. 156-169.

Chen, B.Y., Cheng, X.-P., Kwan, M.-P. & Schwanen, T. (2020). Evaluating spatial accessibility to healthcare services under travel time uncertainty: A reliability-based floating catchment area approach. *Journal of Transport Geography*, 87, 102794.

Chen, P., Tong, R., Lu, G., & Wang, Y. (2018). The α-reliable path problem in stochastic road networks with link correlations: A moment-matching-based path finding algorithm. *Expert Systems with Applications*, 110, 20-32.

Chen, P., Tong, R., Yu, B., & Wang, Y. (2020). Reliable shortest path finding in stochastic time-dependent road network with spatial-temporal link correlations: A case study from Beijing. *Expert Systems with Applications*, 147, 113192.

Dijkstra, E. W. (1959). A note on two problems in connexion with graphs. *Numerische Mathematik*, 1, 269-271.

Engelson, L., & Fosgerau, M. (2016). The cost of travel time variability: Three measures with properties. *Transportation Research Part B*, 91, 555-564.

Faraj, M., & Basir, O. (2016). Optimal energy/time routing in battery-powered vehicles. *2016 IEEE Transportation Electrification Conference and Expo (ITEC),* Dearborn, MI, 1-6. https://doi.org/10.1109/ITEC.2016.7520261.

Frank, H. (1969). Shortest paths in probabilistic graphs. *Operations Research*, 17, 583-599.

`

Frank, R., Castignani, G., Schmitz, R., & Engel, T. (2013). A novel eco-driving application to reduce Energy consumption of electric vehicles. *2013 International Conference on Connected Vehicles and Expo (ICCVE)*, Las Vegas, NV, 283-288. https://doi.org/10.1109/ICCVE.2013.6799807.

Fredman, M.L. & Tarjan, R.E. (1987). Fibonacci heaps and their uses in improved network optimization algorithms. *Journal of the Acm*, 34, 596-615.

Fu, X., Lam, W.H.K., Chen, B.Y. & Liu, Z. (2020). Maximizing space-time accessibility in multi-modal transit networks: an activity-based approach. *Transportmetrica A*, In press.

He, F., Yin, Y. F., & Lawphongpanich, S. (2014). Network equilibrium models with battery electric vehicles. *Transportation Research Part B*, 67, 306-319.

Jafari, E., & Boyles, S. D. (2017). Multi-objective stochastic shortest path problem for electric vehicles. *Networks & Spatial Economics*, 17, 1043-1070.

Ji, Z., Kim, Y. S., & Chen, A. (2011). Multi-objective a-reliable path finding in stochastic networks with correlated link costs: A simulation-based multi-objective genetic algorithm approach (SMOGA). *Expert Systems with Applications*, 38, 1515-1528.

Jiang, Y., & Szeto, W. Y. (2016). Reliability-based stochastic transit assignment: Formulations and capacity paradox. *Transportation Research Part B*, 93, 181-206.

Kaparias, I., Bell, M. G. H., & Belzner, H. (2008). A new measure of travel time reliability for in-vehicle navigation systems. *Journal of Intelligent Transportation Systems*, 12, 202-211.

Kluge, S., Santa, C., Dangl, S., Wild, S., Brokate, M., Reif, K., & Busch, F. (2013). On the computation of the energy-optimal route dependent on the traffic load in Ingolstadt. *Transportation Research Part C*, 36, 97-115.

Kononov, J., Durso, C., Reeves, D., & Allery, B. K. (2012). Relationship between traffic density, speed, and safety and its implications for setting variable speed limits on freeways. *Transportation Research Record: Journal of the Transportation Research Board*, 2280, 1-9.

Lam, T. C., & Small, K. A. (2001). The value of time and reliability: Measurement from a value pricing experiment. *Transportation Research Part E*, 37, 231-251.

Lam, W. H. K., Chan, K. S., & Shi, J. W. Z. (2002). A traffic flow simulator for short-term travel time forecasting. *Journal of Advanced Transportation*, 36, 265-291.

Lam, W. H. K., Shao, H., & Sumalee, A. (2008). Modeling impacts of adverse weather conditions on a road network with uncertainties in demand and supply. *Transportation Research Part B*, 42, 890-910.

Li, Q., Chen, B. Y., Wang, Y., & Lam, W. H. K. (2015). A hybrid link-node approach for finding shortest paths in road networks with turn restrictions. *Transactions in GIS*, 19, 915-929.

Li, Z.-C., Huang, H. J., & Lam, W. H. K. (2012). Modelling heterogeneous drivers' responses to route guidance and parking information systems in stochastic and time-dependent networks. *Transportmetrica*, 8, 105-129.

Nie, Y., & Wu, X. (2009). Shortest path problem considering on-time arrival probability. *Transportation Research Part B*, 43, 597-613.

Quddus, M. A. (2013). Exploring the relationship between average speed, speed variation, and accident rates using spatial statistical models and GIS. *Journal of Transportation Safety & Security*, 5, 27-45.

Raith, A. & Ehrgott, M. (2009). A comparison of solution strategies for biobjective shortest path problems. *Computers & Operations Research*, 36, 1299-1331.

`

Shao, H., Lam, W. H. K., & Tam, M. L. (2006). A reliability-based stochastic traffic assignment model for network with multiple user classes under uncertainty in demand. *Networks & Spatial Economics*, 6, 173-204.
Shen, L., Shao, H., Wu, T., Lam, W. H. K., & Zhu, E. C. (2019). An energy-efficient reliable path finding algorithm for stochastic road networks with electric vehicles. *Transportation Research Part C*, 102, 450-473.
Skriver, A.J.V. (2000). A classification of Bicriterion Shortest Path (BSP) algorithms. *Asia-Pacific Journal of Operational Research*, 17, 199-212.
Srinivasan, K. K., Prakash, A. A., & Seshadri, R. (2014). Finding most reliable paths on networks with correlated and shifted log-normal travel times. *Transportation Research Part B*, 66, 110-128.
Tam, M. L., & Lam, W. H. K. (2008). Using automatic vehicle identification data for travel time estimation in Hong Kong. *Transportmetrica*, 4, 179-194.
Tan, Z., Yang, H., & Guo, R. (2014). Pareto efficiency of reliability-based traffic equilibria and risk-taking behavior of travelers. *Transportation Research Part B*, 66, 16-31.
Taylor, M. C., Lynam, D. A., & Baruya, A. (2000). *The Effects of Drivers' Speed on the Frequency of Road Accidents*. *TRL Report 421*. Transport Research Laboratory, Crowthorne, Berkshire.
Wang, X., Zhou, Q., Quddus, M., Fan, T., & Fang, S. E. (2018). Speed, speed variation and crash relationships for urban arterials. *Accident Analysis and Prevention*, 113, 236-243.
Wu, X., & Nie, Y. (2011). Modeling heterogeneous risk-taking behavior in route choice: a stochastic dominance approach. *Transportation Research Part A*, 45, 896-915.
Yang, S. C., Li, M., Lin, Y., & Tang, T. Q. (2014). Electric vehicle's electricity consumption on a road with different slope. *Physica A*, 402, 41-48.
Yen, J. Y. (1971). Finding the k shortest loop-less paths in a network. *Management Science*, 17, 712-716.
Zhang, R., & Yao, E. (2015). Electric vehicles' Energy consumption estimation with real driving condition data. *Transportation Research Part D*, 41, 177-187.

Appendix

Proposition A1. The standard deviation, $sd_{p_i}^T$, of the underlying normal distribution for any path $p_i^{rs} \epsilon P^{rs}$ satisfies $sd_{p_i}^t \leq sd_{max}^t$, where $sd_{max}^t = max_{a_{ij} \epsilon A}\left(sd_{ij}^T\right)$ is the largest standard deviation of underlying normal distribution for any link on the network.

Proof. For the SD of path travel time, $\sigma_{p_i}^{rs}$, we have $\sigma_{p_i}^{rs} \leq \sum_{a_{ij} \in p_i} \sigma_{ij}^t = \sum_{a_{ij} \in p_i} t_{ij} \frac{\sigma_{ij}^t}{t_{ij}} = \sum_{a_{ij} \in p_i} t_{ij}\, cv_{ij}^t$, where cv_{ij}^t is the coefficient of variation of link travel time. By replacing cv_{ij}^t with $cv_{ij,max}^t$=$max_{a_{ij} \epsilon A}\left(cv_{ij}^t\right)$, the maximal coefficient of variation of travel time on any link a_{ij} in the network, we have $\sigma_{p_i}^{rs} \leq \sum_{a_{ij} \in p_i} t_{ij}\, cv_{ij}^t \leq cv_{ij,max}^t \sum_{a_{ij} \in p_i} t_{ij} = cv_{ij,max}^t t_{p_i}^{rs}$. Since $t_{p_i}^{rs} > 0$, we have $\sigma_{p_i}^{rs}/t_{p_i}^{rs} \leq cv_{ij,max}^t$. Thus, we have $sd_p^t = [\ln\left(1 + (\sigma_{p_i}^{rs})^2/(t_{p_i}^{rs})^2\right)]^{1/2} \leq [\ln\left(1 + \left(cv_{ij,max}^t\right)^2\right)]^{1/2} = sd_{max}^t$. Therefore, $sd_{p_i}^t \leq sd_{max}^t$ holds for any path $p_i^{rs} \epsilon P^{rs}$. □

Proposition A2. The travel time reliability for any path $p_i^{rs} \epsilon P^{rs}$ satisfies $UB\left(R_{p_i}^T\right) \geq R_{p_i}^T$.

`

Proof. According to Proposition A1, we have $sd_{p_i}^t \le sd_{max}^t$ for any *path* $p_i^{rs} \epsilon P^{rs}$. Since $\sigma_{p_i}^{rs} \ge \sigma_{min}^T = min_{p_i \epsilon P^{rs}}(\sigma_{p_i}^{rs})$, we have $(\sigma_{p_i}^{rs})^2/(t_{p_i}^{rs})^2 \ge (\sigma_{min}^T)^2/(t_p^{rs})^2$. Thus, we have $R_{p_i}^T = \Phi\left[\frac{\ln(t_0/t_{p_i}^{rs})}{\left(\ln\left(1+(\sigma_{p_i}^{rs})^2/(t_{p_i}^{rs})^2\right)\right)^{0.5}} + 0.5\, sd_{p_i}^T\right] \le \Phi\left[\frac{\ln(t_0/t_{p_i}^{rs})}{\left(\ln\left(1+(\sigma_{min}^T)^2/(t_{p_i}^{rs})^2\right)\right)^{0.5}} + 0.5 sd_{max}^t\right] = UB(R_{p_i}^T)$. Therefore, we have $R_{p_i}^T \le UB(R_{p_i}^T)$ for any path $\forall p_i^{rs} \epsilon P^{rs}$. □

Proposition A3. The upper bound $UB(R_{p_i}^T)$ of path travel time reliability is a monotonically decreasing function of mean travel time $t_{p_i}^{rs}$ when $t_{p_i}^{rs} > max(\sigma_{min}^T,\ t_0/e)$ holds, where e is Euler's number.
Proof. See the proof of Proposition 2 in Srinivasan, Prakash, and Seshadri (2014). □

Proposition A4. The FindKMRP-TTR procedure can determine the optimal solution of the K most reliable paths for the TTR objective when K_{max} is sufficiently large.
Proof. Suppose that $LB(R_P^T) \ge UB(R_{p_{K1}}^t)$ meets in the first time when k_1 shortest paths were calculated and maintained in $P_{k_1}^t$. Let P^{rs} be the set of all paths between the OD pair, and $\bar{P}^{rs} = P^{rs} - P_{k_1}^t$ be the set of all other paths that have not been calculated between the same OD pair. According to Proposition A3, $UB(R_{p_{k1}}^t)$ is a monotonic decreasing function with respect to the newly calculated kth shortest path. Thus, we have $LB(R_P^T) \ge UB(R_{p_{k1}}^t) \ge UB(R_{p_i}^t) \ge R_{p_i}^t$ for $\forall p_i^{rs} \in \bar{P}^{rs}$. Since $LB(R_P^T) = max_{p_i \epsilon P_{k_1}^t}(R_{p_i}^t)$, we have $LB(R_P^T) \ge R_{p_i}^t$ for $\forall p_i^{rs} \in P_{k_1}^t$. Thus, we have $LB(R_P^T) \ge R_{p_i}^t$ for $\forall p_i^{rs} \in P^{rs}$. Therefore, path p_{LB}^T providing the lower bound $LB(R_P^T)$ was the first most reliable path for the TTR objective.
Without loss of generality, it is assumed that j (j=1, …, or $K^T - 1$) most reliable paths have been determined and maintained in P^T when k_j shortest paths were calculated. Let $P_{k_j}^t$ be the set of calculated k_j shortest paths excluding P^T. Thus, we have $R_{p_w}^t \ge R_{p_i}^t$ for $\forall p_w^{rs} \in P^T$ and $\forall p_i^{rs} \in P_{k_j}^t$. It is assumed $LB(R_P^T) \ge UB\left(R_{p_{Kj+1}}^t\right)$ holds again when k_{j+1} shortest paths were calculated. Let $P_{k_{j+1}}^t$ be the set of calculated k_{j+1} shortest paths excluding P^T. According to Proposition A3, we have $R_{p_w}^t \ge R_{p_i}^t$ for $\forall p_w^{rs} \in P^T$ and $\forall p_i^{rs} \in P_{k_{j+1}}^t$. Therefore, $R_{p_w}^t \ge LB(R_P^T)$ for $\forall p_w^{rs} \in P^T$. Let $\bar{P}^{rs} = P^{rs} - P_{k_{j+1}}^t - P^T$ be the set of all other paths that have not been calculated between the same OD pair. According to Proposition A3, we have $LB(R_P^T) \ge UB\left(R_{p_{Kj+1}}^t\right) \ge UB(R_{p_i}^t) \ge R_{p_i}^t$ for $\forall p_i^{rs} \in \bar{P}^{rs}$. Since $LB(R_P^T) = max_{p_i \epsilon P_{k_{j+1}}^t}(R_{p_i}^t)$, we have $LB(R_P^T) \ge R_{p_i}^t$ for $\forall p_i^{rs} \in P_{k_{j+1}}^t$. Therefore, we have $LB(R_P^T) \ge R_{p_i}^t$ for $\forall p_i^{rs} \in P^{rs} - P^T$. Therefore, path p_{LB}^T providing the lower bound $LB(R_P^T)$ was the j+1th most reliable path for the TTR objective. □

Proposition A5. The FindTtrEcrPathSet algorithm can determine the optimal solution of the bi-objective reliable PFP when K_{max} is sufficiently large.
Proof. Let Θ be the optimal solution containing all non-dominated paths between the OD pair. Without loss of generality, it is assumed that the algorithm terminates when $R_{R_j}^T < R_{Min}^T$ holds, where R_{Min}^T is the actual TTR of $p_{R_1}^C$, the most reliable path in terms of the ECR objective. Let P^T be the set of calculated j most reliable paths, and $\bar{P}^{rs} = P^{rs} - P^T$ be the set of all other paths that

`

have not been calculated between the same OD pair. According to the definition of K most reliable paths of the TTR objective, we have $R^T_{R_j} \geq R^T_{R_i}$ for any $p^{rs}_i \in \bar{P}^{rs}$. Therefore, we have $R^T_{Min} > R^T_{R_j} \geq R^T_{R_i}$ for any $p^{rs}_i \in \bar{P}^{rs}$. According to the definition of the most reliable, we have $R^C_{p_1} = max_{p_i \epsilon P^{rs}}\left(R^C_{p_i}\right)$, and thus $R^C_{p_1} \geq R^C_{R_i}$ for any $p^{rs}_i \in \bar{P}^{rs}$. Thus, all paths in $\bar{P}^{rs}$ are dominated by $p^C_{R_1}$. Therefore, we have $\Theta \subset P^T$. For paths in P^T, the algorithm eliminates any path, $p^T_{R_j}$, with $R^C_{R_j} \leq R^C_{R_{j-1}}$ (see Line 12), and maintains other paths in Ω (see Line 13). Because $R^T_{R_j} < R^T_{R_{j-1}}$ and $R^C_{R_j} \leq R^C_{R_{j-1}}$ hold, the eliminated path $p^T_{R_j}$ is dominated by $p^T_{R_{j-1}}$. Therefore, we have $\Theta \subset \Omega$. In the algorithm, paths are added into Ω in a descending order of the TTR value but an ascending order of the ECR value. Thus, we have $R^T_{R_1} \geq \cdots \geq R^T_{R_j}$ and $R^C_{R_1} \leq \cdots \leq R^C_{R_j}$ for all paths in Ω. Then, each path $p^{rs}_i \in \Omega$ is not dominated by any other path $p^{rs}_w \in \Omega$. According to Definition 2, all paths in Ω are non-dominated paths. Thus, we have $\Omega \subset \Theta$. Therefore, we have $\Omega = \Theta$. □